

The *effective spin* concept
to analyze coherent charge transport
in mesoscopic systems

J. Wan, W. Liu, M. Cahay

Department of Electrical and Computer Engineering
University of Cincinnati, Cincinnati, Ohio 45221

V. Gasparian

Department of Physics, California State University, Bakersfield, CA 93311

S. Bandyopadhyay

Department of Electrical and Computer Engineering
Virginia Commonwealth University, Richmond, Virginia 23284

June 23, 2018

Abstract

An *effective spin* concept is introduced to examine the mathematical and physical analogy between phase coherent charge transport in mesoscopic systems and quantum operations on spin based qubits. When coupled with the Bloch sphere concept, this isomorphism allows formulation of transport problems in a language more familiar to researchers in the field of spintronics and quantum computing. We exemplify the synergy between charge tunneling and spin qubit unitary operations by recasting well-known problems of tunneling through a delta scatterer, a resonant tunneling structure, a superlattice structure, and arrays of elastic scatterers, in terms of specific unitary operations (rotations) of a spinor on the Bloch sphere.

PACS: 73.23.Ad,03.65.Nk,03.67.Lx,76.60.-k

I. Introduction

Two major areas of research in condensed matter physics are phase coherent charge transport in mesoscopic structures [1, 2, 3] and spin based quantum computing [4, 5, 6, 7, 8, 9, 10, 11]. These two areas are seemingly disparate and until recently have evolved independently. Some efforts to stress analogies between the two fields have appeared recently [12, 13]. In this paper, we investigate and develop further the isomorphism between these two areas by introducing an *effective spin* concept to describe phase coherent charge transport through two-dimensional arrays of elastic scatterers.

In tunneling problems, the mesoscopic structure through which an electron tunnels, is characterized by an arbitrary potential barrier. The transmission and reflection amplitudes are usually calculated by the so-called “scattering matrix approach” [14, 15]. The scattering matrix relates the incoming (a^+, b^-) to outgoing wave amplitudes (b^+, a^-) on both sides of a scattering region (mesoscopic structure), as shown in Figure 1, such that

$$|\psi(OUT)\rangle = \begin{bmatrix} b^+ \\ a^- \end{bmatrix} = S \begin{bmatrix} a^+ \\ b^- \end{bmatrix} = \begin{bmatrix} t & r' \\ r & t' \end{bmatrix} \begin{bmatrix} a^+ \\ b^- \end{bmatrix} = S |\psi(IN)\rangle, \quad (1)$$

where S is the scattering matrix.

For single-mode transport, assuming an electron incident from the left,

$$|\psi^l(IN)\rangle = \begin{bmatrix} 1 \\ 0 \end{bmatrix}, \quad (2)$$

and

$$|\psi^l(OUT)\rangle = \begin{bmatrix} t \\ r \end{bmatrix}, \quad (3)$$

whereas, for an electron incident from the right, we have

$$|\psi^r(IN)\rangle = \begin{bmatrix} 0 \\ 1 \end{bmatrix}, \quad (4)$$

and

$$|\psi^r(OUT)\rangle = \begin{bmatrix} r' \\ t' \end{bmatrix}. \quad (5)$$

The tunneling problem is completely characterized by the amplitudes (t, r) or (r', t') depending on the direction of incidence of the incoming electron.

Without any loss of generality, we can always think of the two-component column vector $|\psi(OUT)\rangle$ as a spinor, since it is normalized in the case of coherent transport. The normalization follows from the unitarity of the scattering matrix, i.e., $S^\dagger S = I$. Furthermore, the spinor $|\psi(OUT)\rangle$ can be thought as the output of a one-qubit quantum gate whose input is the spinor $|\psi(IN)\rangle = (1, 0)^\dagger$ or $(0, 1)^\dagger$ (where \dagger stands for Hermitian conjugate) depending on the direction of propagation of the incident electron. The 2×2 unitary matrix linking the spinors $|\psi(IN)\rangle$ and $|\psi(OUT)\rangle$ can therefore be viewed as the matrix characterizing rotation of a qubit whose initial state was $|\psi(IN)\rangle$ and whose final state becomes $|\psi(OUT)\rangle$. This matrix is also the scattering matrix describing the tunneling problem. Herein lies the analogy between quantum logic operation on a spin qubit and coherent charge transport in a mesoscopic structure. This paper explores this analogy for single channel charge tunneling through a single delta-scatterer, a resonant tunneling structure, a periodic array of delta scatterers, and one-dimensional arrays of randomly distributed elastic scatterers.

II. Theory

Consider the tunneling problem of an electron incident from the left on an arbitrary one-dimensional conduction band energy profile $E_c(x)$. We refer to the (2×1) column vector $|\psi^l(OUT)\rangle$ in Equation (3) as the *effective spin* whose components characterize completely the scattering am-

plitudes of the tunneling electron. For an arbitrary potential energy profile $E_c(x)$, the amplitude $|\psi^l(OUT)\rangle$ can be found by successively cascading scattering matrices associated with “subsections” within each of which $E_c(x)$ is approximated by constant values $E_{c1}, E_{c2}, E_{c3} \dots E_{cn}$ [14, 15]. The evolution of the pure state $|\psi^l(OUT)\rangle$ after crossing a number of subsections can be represented using the Bloch sphere concept in which the spinor is parameterized as follows [16, 17]

$$|\psi^l(OUT)\rangle = e^{i\gamma} \left[\cos \frac{\theta}{2} |0\rangle + \sin \frac{\theta}{2} e^{i\varphi} |1\rangle \right], \quad (6)$$

where γ is an arbitrary phase factor and the angles (φ, θ) are the azimuthal and polar angles, as shown in Figure 2.

In Equation (6), $|0\rangle$ and $|1\rangle$ are the (2×1) column vectors $(1, 0)^\dagger$ and $(0, 1)^\dagger$ respectively, associated with the north and south poles of the Bloch sphere. They are mutually orthogonal, i.e., their inner product $\langle 0|1 \rangle = 0$ [16].

To complete the effective spin picture, we consider the following 2×2 matrix [18]

$$\rho = |\psi^l(OUT)\rangle \langle \psi^l(OUT)| = \begin{pmatrix} t \\ r \end{pmatrix} (t^* r^*) = \begin{pmatrix} |t|^2 & tr^* \\ rt^* & |r|^2 \end{pmatrix}. \quad (7)$$

Using this density matrix and the Pauli spin matrices $(\sigma_x, \sigma_y, \sigma_z)$, the effective “spin components” associated with the spinor $|\psi^l(OUT)\rangle$ are given by

$$\langle S_x \rangle = \frac{\hbar}{2} \text{Tr}(\rho \sigma_x) = \frac{\hbar}{2} (tr^* + rt^*) = \hbar \text{Re}(rt^*) = \hbar \text{Re}(r^*t), \quad (8)$$

$$\langle S_y \rangle = \frac{\hbar}{2} \text{Tr}(\rho \sigma_y) = \frac{\hbar}{2} i (tr^* - rt^*) = \hbar \text{Im}(rt^*) = -\hbar \text{Im}(r^*t), \quad (9)$$

and

$$\langle S_z \rangle = \frac{\hbar}{2} \text{Tr}(\rho \sigma_z) = \frac{\hbar}{2} (|t|^2 - |r|^2) = \frac{\hbar}{2} (1 - 2|r|^2) = \frac{\hbar}{2} (2|t|^2 - 1). \quad (10)$$

For an electron incident from the right, $|\psi^r(IN)\rangle = |1\rangle$, and the density matrix ρ' ($=|\psi^r(OUT)\rangle\langle\psi^r(OUT)|$) is such that $\rho' = 1 - \rho$, where ρ is given by Equation (7) and the components $\langle S_x \rangle$, $\langle S_y \rangle$ and $\langle S_z \rangle$ are just the negative of the values in Equations (8-10). Therefore the two spinors corresponding to $|\psi^l(OUT)\rangle$ and $|\psi^r(OUT)\rangle$ are mirror images of each other, corresponding to a reflection through the origin of the Bloch sphere. This means that $|\psi^l(OUT)\rangle$ and $|\psi^r(OUT)\rangle$ are orthogonal, which they must be because the scattering matrix is unitary.

The unitarity of the scattering matrix also leads to:

$$\langle S_x \rangle^2 + \langle S_y \rangle^2 = \hbar^2 |t|^2 (1 - |t|^2), \quad (11)$$

and

$$\langle S_x \rangle^2 + \langle S_y \rangle^2 + \langle S_z \rangle^2 = \hbar^2 / 4. \quad (12)$$

Equation (11) shows that the projection of the spinor in the equatorial plane of the Bloch sphere reaches a maximum when $|t| = |r| = 1/\sqrt{2}$. Actually, $\langle S_x \rangle^2 + \langle S_y \rangle^2$ is proportional to $|t|^2 (1 - |t|^2)$, i.e., the low frequency shot noise power for the tunneling electron [19]. Since $(\langle S_x \rangle, \langle S_y \rangle, \langle S_z \rangle)$ are proportional to the components of the spinor $|\psi(OUT)\rangle$ on the Bloch sphere, Equation (12) simply states that the spinor stays on the Bloch sphere during cascading of scattering matrices. This is expected for the case of coherent transport. The angles $(\gamma, \theta, \varphi)$ appearing in the generic expression of the spinor (or qubit) in Equation (6) can be expressed in terms of the phases

and magnitudes of the reflection and transmission coefficients:

$$|\psi^l(OUT)\rangle = \begin{bmatrix} t \\ r \end{bmatrix} = \begin{bmatrix} |t|e^{i\phi_T} \\ |r|e^{i\phi_R} \end{bmatrix} = e^{i\phi_T} \begin{bmatrix} |t| \\ |r|e^{i(\phi_R-\phi_T)} \end{bmatrix}. \quad (13)$$

where ϕ_R and ϕ_T are the phases of the reflection and transmission amplitudes, respectively.

We get

$$\gamma = \phi_T, \quad (14)$$

and

$$\varphi = \phi_R - \phi_T. \quad (15)$$

Furthermore,

$$|t| = \cos \frac{\theta}{2}, \quad (16)$$

$$|r| = \sin \frac{\theta}{2} = \sqrt{1 - |t|^2}, \quad (17)$$

and therefore,

$$\frac{\theta}{2} = \tan^{-1} \left(\frac{|r|}{|t|} \right). \quad (18)$$

Equations (8-10) are therefore equivalent to

$$\langle S_x \rangle = \frac{\hbar}{2} \sin \theta \cos \varphi, \quad (19)$$

$$\langle S_y \rangle = \frac{\hbar}{2} \sin \theta \sin \varphi, \quad (20)$$

and

$$\langle S_z \rangle = \frac{\hbar}{2} \cos \theta, \quad (21)$$

Equations (8) and (9) clearly show that the averages $\langle S_x \rangle$ and $\langle S_y \rangle$ contain more information than the sample conductance alone. The latter depends only on the magnitude of transmission $|t|$ or reflection $|r|$ in the Landauer picture [20], whereas $\langle S_x \rangle$ and $\langle S_y \rangle$ depend on the phase relationship between t and r as well. The phase relationship is a strong function of the energy of the incident electron. At non zero temperature, there will be a thermal spread in the energy of the incident electron which will lead to a rapid wash out with temperature of the components $\langle S_x \rangle$ and $\langle S_y \rangle$, i.e., the off-diagonal components of the density matrix ρ . Note that while $\langle S_x \rangle$ and $\langle S_y \rangle$ depend on the off-diagonal components of the density matrix and are very energy sensitive, $\langle S_z \rangle$ depends only on the diagonal components of the density matrix and is much less energy sensitive.

II.1 Quantum computing gate analog

The 2×2 unitary matrix or quantum computing gate U_{QG} which relates $|\psi(OUT)\rangle$ and $|\psi(IN)\rangle$ on the Bloch sphere has the general form [16]

$$U_{QG}(\alpha, \beta, \eta, \zeta) = e^{i\alpha} R_z(\beta) R_y(\eta) R_z(\zeta), \quad (22)$$

where $(\alpha, \beta, \eta, \zeta)$ are real numbers and the R_y and R_z are the 2×2 matrices associated with rotations of the spinor on the Bloch sphere about the \hat{y} and \hat{z} axis, respectively. Using the fact that $R_y(\eta) =$

$e^{-i\frac{\eta}{2}\sigma_y}$ and $R_z(\zeta) = e^{-i\frac{\zeta}{2}\sigma_z}$ [16], we obtain:

$$U_{QG}(\alpha, \beta, \eta, \zeta) = \begin{bmatrix} e^{i(\alpha - \frac{\beta - \zeta}{2})} \cos \frac{\eta}{2} & -e^{i(\alpha - \frac{\beta + \zeta}{2})} \sin \frac{\eta}{2} \\ e^{i(\alpha + \frac{\beta - \zeta}{2})} \sin \frac{\eta}{2} & e^{i(\alpha + \frac{\beta + \zeta}{2})} \cos \frac{\eta}{2} \end{bmatrix}. \quad (23)$$

For $|\psi^l(IN)\rangle = |0\rangle$, we have

$$|\psi^l(OUT)\rangle = U_{QG}(\alpha, \beta, \eta, \zeta)|0\rangle = \begin{bmatrix} e^{i(\alpha - \frac{\beta - \zeta}{2})} \cos \frac{\eta}{2} \\ e^{i(\alpha + \frac{\beta - \zeta}{2})} \sin \frac{\eta}{2} \end{bmatrix}, \quad (24)$$

which is the special case of a spinor on the Bloch sphere in Equation (6), corresponding to

$$\begin{aligned} \alpha &= \gamma = \phi_T, \\ \eta &= \theta = 2 \tan^{-1} \left[\frac{|r|}{|t|} \right], \\ \beta &= -\zeta = \varphi = \phi_R - \phi_T. \end{aligned} \quad (25)$$

Hence, from a quantum computing perspective, the analytical expression for U_{QG} is identical to the scattering matrix used to describe the tunneling problem and is given explicitly by

$$U_{QG}(\phi_T, \theta, |t|) = e^{i\phi_T} R_z(\phi_R - \phi_T) R_y \left(2 \tan^{-1} \left[\frac{|r|}{|t|} \right] \right) R_z(\phi_T - \phi_R), \quad (26)$$

This last equation helps visualizing coherent charge transport (or tunneling) through specific mesoscopic devices as a successive set of rotations of the effective spin on the Bloch sphere, as will be illustrated in the numerical examples in section III.

In the next section, we provide several examples to illustrate the *effective spin* concept.

III. Examples

III.1 Scattering across a single delta scatterer

We first determine the quantum computing gate analog of a simple delta scatterer of strength $V_I\delta(x)$ for which the reflection and transmission amplitudes are easily shown to be

$$t' = t = \frac{ik}{ik - k_0} = \frac{\widetilde{ik}}{\widetilde{ik} - 1}, \quad (27)$$

and

$$r' = r = \frac{k_0}{ik - k_0} = \frac{1}{\widetilde{ik} - 1}, \quad (28)$$

with $\widetilde{k} = k/k_0$, $k_0 = m^*V_I/\hbar^2$ and $k = \frac{\sqrt{2m^*E}}{\hbar}$, where E is the kinetic energy of the electron and m^* is its effective mass.

The magnitude and phase of t and r are therefore

$$|t| = \frac{\widetilde{k}}{\sqrt{\widetilde{k}^2 + 1}}, \phi_T = -\tan^{-1}\left(\frac{1}{\widetilde{k}}\right), \quad (29)$$

and

$$|r| = \frac{1}{\sqrt{\widetilde{k}^2 + 1}}, \phi_R = \tan^{-1}\left(\widetilde{k}\right) - \pi. \quad (30)$$

The spinor $|\psi^l(OUT)\rangle$ for this simple problem is given by Equation (6), where

$$\varphi = \phi_R - \phi_T = -\frac{\pi}{2}, \quad (31)$$

and

$$\theta = 2 \tan^{-1}\left(1/\widetilde{k}\right). \quad (32)$$

The equivalent quantum computing gate is characterized by unitary matrix U_{QG} given by

$$U_{QG} = e^{i\varphi_T} R_z\left(\frac{-\pi}{2}\right) R_y(\theta) R_z\left(\frac{\pi}{2}\right) = e^{i\varphi_T} R_x(-\theta), \quad (33)$$

where R_x is the matrix for spinor rotation around the x-axis [16]. For low incident energy, $\theta = \pi$ and it monotonically goes to 0 as the energy of the incident electron increases. According to Eqns.(19-21), the spinor $|\psi^l(OUT)\rangle$ sweeps only a very limited portion of the Bloch sphere, i.e., the semi-circle in the y-z plane, going from the south to north poles clockwise as the energy of the incident electron increases. The spin components of $|\psi^l(OUT)\rangle$ along the x, y, and z axes are given by

$$\langle S_x \rangle = 0, \quad (34)$$

$$\langle S_y \rangle = -\frac{\hbar}{2} \left(\frac{2\tilde{k}}{\tilde{k}^2 + 1} \right), \quad (35)$$

and

$$\langle S_z \rangle = \frac{\hbar}{2} \left(\frac{\tilde{k}^2 - 1}{\tilde{k}^2 + 1} \right). \quad (36)$$

For instance, when $\tilde{k} = 1$, $|\psi^l(OUT)\rangle$ is in the equatorial plane of the Bloch sphere, along the y-axis. In this case, $\theta = \frac{\pi}{2}$, and the matrix U_{QG} is given by

$$U_{QG} = e^{-i\frac{\pi}{4}} R_z\left(-\frac{\pi}{2}\right) R_y\left(\frac{\pi}{2}\right) R_z\left(\frac{\pi}{2}\right) = e^{-i\frac{\pi}{4}} S\left(-\frac{\pi}{2}\right) \sigma_x \mathcal{H} S\left(\frac{\pi}{2}\right), \quad (37)$$

where

$$S(\delta) = \begin{bmatrix} 1 & 0 \\ 0 & e^{i\delta} \end{bmatrix}, \quad (38)$$

and

$$\mathcal{H} = \frac{1}{\sqrt{2}} \begin{bmatrix} 1 & 1 \\ 1 & -1 \end{bmatrix}, \quad (39)$$

are the general phase shift and the Hadamard matrix, respectively, extensively used in the theory of quantum computing [16].

III.2 Scattering through a delta-scatterer in a region of length a

Next, we consider the scattering problem across a region of length a containing a delta scatterer at location x_0 . The corresponding scattering matrix can be easily derived. The location of the spinor $|\psi^l(OUT)\rangle$ on the Bloch sphere is described by azimuthal angle θ given in Equation (21) and polar angle

$$\varphi = \frac{-\pi}{2} - k(a - 2x_0). \quad (40)$$

The average values of the effective spin components are given by

$$\langle S_x \rangle = \frac{\hbar}{2} \left(\frac{2\tilde{k}}{\tilde{k}^2 + 1} \right) \sin k(2x_0 - a), \quad (41)$$

$$\langle S_y \rangle = - \frac{\hbar}{2} \left(\frac{2\tilde{k}}{\tilde{k}^2 + 1} \right) \cos k(2x_0 - a), \quad (42)$$

$$\langle S_z \rangle = \frac{\hbar}{2} \left(\frac{\tilde{k}^2 - 1}{\tilde{k}^2 + 1} \right). \quad (43)$$

In this case, $\langle S_x \rangle$ is non-zero unless $x_0 = \frac{a}{2}$, i.e., unless the potential energy profile in the device is spatially symmetric. For a fixed value of the incident wavevector, the spinor $|\psi^l(OUT)\rangle$ moves on a circle parallel to the (x, y) plane. If a is selected such that $ka = \pi$, φ increases linearly from $-\frac{3\pi}{2}$ to $\frac{\pi}{2}$ as x_0 varies from 0 to a , i.e., the Bloch vector associated with the spinor sweeps the entire plane defined by the component $\langle S_z \rangle$. According to Eqns.(41) and (42), if $ka = \pi$, the

average value of $\langle S_x \rangle$ and $\langle S_y \rangle$ are equal to zero when we average over the impurity location x_0 . This is an important ingredient in the theory of localization in 1D arrays of scatterers, as will be discussed later. The quantum computing gate U_{QG} analog of this tunneling problem is given by

$$U_{QG} = e^{i\phi_T} R_z\left(-\frac{\pi}{2} + k(2x_0 - a)\right) R_y(\theta) R_z\left(k(a - 2x_0) + \frac{\pi}{2}\right). \quad (44)$$

Since θ is still given by Equation (21), a *spin flip* from the south to north pole is only possible if we increase the energy of the incident electron to infinity. The energy cost for the spin flip is drastically reduced if we have two or more delta scatterers, as discussed next.

III.3 Scattering across a resonant tunneling structure

We consider the scattering problem across a resonant tunneling structure consisting of two delta scatterers of equal strength V_I separated by a distance a . In our numerical simulations, we use $V_I = 0.3eV\text{\AA}$ and $a = 50 \text{\AA}$. Figure 3 is a plot of the transmission coefficient T as a function of the reduced wavevector \tilde{k} . The first two resonances (at which $T = 1$) occur at $\tilde{k} \approx 12.5$ and 36 . The corresponding variation of the phase angles (φ, θ) for the spinor $|\psi^l(OUT)\rangle$ are displayed in Figure 4. The angle θ reaches its minimum value of zero at the resonances when there is a sudden jump in φ . When viewed as a quantum computing gate, an RTD is more efficient when operated over the range $\Delta\tilde{k}$ indicated in Figure 4 since it allows a full swing in θ from 0 to π , whereas the swing in θ is much smaller between the first two and higher resonances. The quantity $\Delta\tilde{k}$ is much smaller than the infinite change in \tilde{k} needed for a single delta-scatterer to realize an inverter, as discussed in the previous section. Since $T = R$ for $\tilde{k} = \tilde{k}^*$, $\theta = \frac{\pi}{2}$ which is enough to implement the Hadamard gate using an RTD.

The results above can be extended to the case of a superlattice, modeled as a sequence of evenly spaced identical delta scatterers. In that case, each resonant state present in the smaller unit with two scatterers (RTD) leads to a passband for the infinitely periodic structure. In Figure 5, we plot the transmission coefficient for a structure consisting of 5 delta scatterers with the same parameters as for the RTD described above and with the same spacing of 50\AA between each

scatterer. The transmission coefficient reaches unity at four values of \tilde{k} in the interval $[5 - 25]$, which is a well known result for finite repeated structures [23, 24]. Furthermore, the range $\Delta\tilde{k}$ needed to reach the condition $T = R$ is reduced compared to the case of a RTD. As the number of periods in the superlattice increase, $\Delta\tilde{k}$ actually converges to a limit corresponding to the lower edge of the pass band of the infinite superlattice. As shown in Figure 6, the angle θ allows a full swing from north to south poles on the Bloch sphere over a range $\Delta\tilde{k}$ smaller than what is necessary for the case of the RTD, and the phase angle φ toggles back and forth between $-\frac{\pi}{2}$ and $\frac{\pi}{2}$ each time a resonance is crossed.

Figure 5 also shows a plot of the transmission coefficient (curves labeled 1 and 2) versus \tilde{k} for two imperfect structures, in which the locations of the five delta scatterers are selected randomly and uniformly over each interval of length a . The transmission coefficient is fairly sensitive to \tilde{k} in the range of \tilde{k} where the lower pass band will develop for the infinite superlattice. However, the transmission curve is fairly insensitive to the imperfections in the superlattice in the same range of \tilde{k} . As shown in Figure 6, the angle θ is also fairly insensitive to imperfections in the superlattice but the phase φ is not. The latter result is a compounded effect of multiple reflections between impurities and the sensitivity of φ to the exact impurity location in each section of length a , as discussed earlier.

III. 4 Scattering through a periodic array of delta scatterers

The scattering matrix elements for 1D periodic system (or superlattice) can be calculated exactly [25, 26, 27]. The transmission amplitude is found to be

$$t_N = \frac{e^{i(N-1)ka}}{D_N}, \quad (45)$$

and the reflection amplitude is given by

$$r_N = -i \frac{k_0}{k} \frac{e^{i(N-1)ka}}{D_N} \frac{\sin(N\beta a)}{\sin(\beta a)}, \quad (46)$$

where

$$D_N = e^{iNka} \left\{ \cos(N\beta a) + i \operatorname{Im} \left[e^{-ika} \left(1 + i \frac{k_0}{k} \right) \right] \frac{\sin(N\beta a)}{\sin(\beta a)} \right\} \quad (47)$$

and $k = \frac{1}{\hbar} \sqrt{2m^*E}$, $k_0 = m^*V_I/\hbar^2$, a is the distance between adjacent scatterers, and β is the quasi momentum. It is the solution of the transcendental equation:

$$\cos(\beta a) = \cos(ka) + \frac{k_0}{k} \sin(ka). \quad (48)$$

Using Eqs.(8-10), it can be shown that $\langle S_x \rangle = 0$ and

$$\langle S_y \rangle = -\hbar \operatorname{Re}(r^*t) = -\frac{\hbar}{1 + \left(\frac{k_0}{k}\right)^2 \frac{\sin^2(N\beta a)}{\sin^2(\beta a)}} \frac{\sin(N\beta a)}{\sin(\beta a)} \frac{k_0}{k}, \quad (49)$$

and

$$\langle S_z \rangle = \frac{\hbar}{2} (2|t|^2 - 1) = \frac{\hbar}{2} \left[\frac{2}{1 + \left(\frac{k_0}{k}\right)^2 \frac{\sin^2(N\beta a)}{\sin^2(\beta a)}} - 1 \right]. \quad (50)$$

In the case of $N = 1$, we get back Eqs. (35) and (36) of section III.1. In the case of N delta scatterers, incident energies for which

$$\frac{\sin(N\beta a)}{\sin(\beta a)} = 0, \quad (51)$$

correspond to points of unity transmission which occur at values of the quasi-momentum in the first Brillouin zone

$$\beta_n a = \frac{\pi n}{N} \quad (52)$$

with $(n = 1, \dots, N - 1)$.

At these values, $\langle S_x \rangle = \langle S_y \rangle = 0$ and $\langle S_z \rangle = \frac{\hbar}{2}$.

III.5 Transport through random arrays of delta scatterers

The analysis of the previous section was extended to a large number of delta scatterers of strength $V_I \delta(x - (x_0^i + (i - 1)a))$, where V_I is selected to be $0.3 \text{ eV}\text{\AA}$ and x_0^i is the location of the i^{th} impurity

located in the interval $[(i - 1)a, ia]$ Each impurity location is generated using a uniform random number in each interval. The length of each subsection is set equal to 237 \AA and the wavevector of the incident electron $k = \frac{\sqrt{2m^*E}}{\hbar}$, is selected such that $ka = \pi$, for an incident energy E of 10 meV and $m^* = 0.067m_0$, the electron effective mass in GaAs.

Figure 7 is a plot of the phase angle θ of the spinor $|\psi^l(OUT)\rangle$ versus the number of subsections (N) crossed. The two top curves are θ versus N for two specific impurity configurations. The curves show regions where θ decreases as N increases which corresponds to an increase in the conductance of the array. This decrease in θ as N increases is quite pronounced for one of the two impurity configurations, for $N < 20$. A plot of the average value of θ over an ensemble of 10^5 samples is shown as the curve labeled $\bar{\theta}$ in Figure 7. The quantity $\bar{\theta} = \pi/2$ for $N \approx 23$. This corresponds to a conductance of e^2/h , as shown in Figure 8, and to an elastic mean free path equal to $23 \times 237 \text{ \AA} \sim 0.55 \mu\text{m}$.

IV. Conclusions

The effective spin concept examined in this paper offers an alternative description of phase coherent charge transport through mesoscopic systems in terms familiar to researchers in the field of spintronics and quantum computing. As illustrated in this paper, the effective spin formalism provides a pedagogical approach to simple scattering problems and also to the phenomenon of localization in random arrays of elastic scatterers.

In the past, the effective spin concept has been used to describe the spatial correlations between reflection and transmission amplitudes of polarized photon beams from a combination of beam splitters, mirrors, and interferometers [31, 32, 33]. More recently, the effective spin concept has been used to examine the critical problem of entanglement between channels associated with propagating modes in mesoscopic systems, as reported in recent experiments by Neder et al. [12] and their theoretical interpretation by Samuelson et al. [34].

References

- [1] Y. Imry, *Introduction to Mesoscopic Physics*, (Oxford University Press, 2002).
- [2] M. Cahay and S. Bandyopadhyay, in *Advances in Electronics and Electron Physics*, Vol. 89, Ed. P. W. Hawkes, (Academic Press, San Diego, 1994). p. 94.
- [3] C. W. J. Beenakker and H. van Houten, in *Solid State Physics*, Vol. 44, Eds. H. Ehrenreich and D. Turnbull, (Academic Press, Boston, 1991). p. 1.
- [4] S. Bandyopadhyay and V. P. Roychowdhury, *Superlat. Microstruct.* **22**, 411 (1997).
- [5] L. A. Openov and A. M. Bychkov, *Phys. Low Dim. Struct.* **9-10**, 153 (1998). Also available as www.arXiv.org/cond-mat/9809112.
- [6] D. Loss and D. P. DiVincenzo, *Phys. Rev. A* **57**, 120 (1998).
- [7] V. Privman, I. D. Wagner and G. Kventsel, *Phys. Lett. A* **239**, 141 (1998).
- [8] B. E. Kane, *Nature (London)* **393**, 133 (1998).
- [9] S. Bandyopadhyay, *Phys. Rev. B* **61**, 13813 (2000).
- [10] T. Calarco, A. Datta, P. Fedichev and P. Zoller, *Phys. Rev. A* **68**, 012310 (2003).
- [11] A. E. Popescu and R. Ionicioiu, *Phys. Rev. B* **69**, 245422 (2004).
- [12] See I. Neder, N. Ofek, Y. Chung, M. Heiblum, D. Mahalu, and V. Umansky, *Nature* 448, 333 (2007) and references therein.
- [13] R. Ionicioiu, *Spintronics devices as quantum networks*, [quant-ph/0512116](http://arXiv.org/abs/quant-ph/0512116).
- [14] S. Datta, M. Cahay and M. McLennan, *Phys. Rev. B* **36**, 5655 (1987).
- [15] M. Cahay, M. McLennan and S. Datta, *Phys. Rev. B* **37**, 10125 (1988).

- [16] M. A. Nielsen and I. L. Chuang, *Quantum computation and quantum information* (Cambridge University Press, NY, 2000).
- [17] S. Bandyopadhyay and M. Cahay, *Introduction to Spintronics* (CRC Press, Boca Raton, 2008).
- [18] Using the unitary property of the scattering matrix, it can be easily checked that the trace of the matrix ρ is unity and ρ satisfies the following properties, $\rho^\dagger = \rho$, $\rho^2 = \rho$, and $Tr[\rho^2] = Tr[\rho] = 1$, which are all characteristic of the density matrix associated with a pure state [16].
- [19] Y. M. Blanter and M. Büttiker, Phys. Rep. **336**, 1, (2000).
- [20] R. Landauer, IBM J. Res. Dev. **1**, 223 (1957).
- [21] P. A. Lee and T. V. Ramakrishnan, Rev. Mod. Phys. **57**, 287 (1985).
- [22] P. Erdos and R.C. Herndon, Adv. Phys. **31**, 65 (1982).
- [23] D.J. Vezzetti and M. Cahay, J. Phys. D: Appl. Phys., **19**, L53-L55 (1986).
- [24] M. Cahay and S. Bandyopadhyay, Phys. Rev. B **42**, 5100 (1990).
- [25] V. M. Gasparian, B. L. Altshuler, A. G. Aronov, and Z. H. Kasamian, Phys. Lett. A **132**, 201 (1988).
- [26] V. Gasparian, Sov. Phys. Solid State **31** (2), 266 (1989); Fizika Tverdogo Tela **31** (2), 162 (1989).
- [27] V. Gasparian, U. Gummich, E. Jódar, J. Ruiz and M. Ortuño, Physica B, **233**, 72 (1997).
- [28] M. Cahay, S. Bandyopadhyay, M.A. Osman, and H.L. Grubin, Surf. Sci. **228**, 301 (1990).
- [29] P.F. Bagwell, Phys. Rev. B **41**, 10354 (1990).
- [30] A. D. Stone and P. A. Lee, Phys. Rev. Lett, **54**, 1196 (1985).

- [31] C. H. Holbrow, E. J. Galvez, and M. E. Parks, *Am. J. Phys.* **70**, 260C265 (2002)
- [32] T. B. Pittman, B. C. Jacobs, and J. D. Franson, *Phys. Rev. A* **64**, 062311 (2001).
- [33] P. T. Cochrane and G. J. Milburn, *Phys. Rev. A* **64**, 062312 (2001)
- [34] P. Samuelson, I. Neder, and M. Büttiker, *Phys. Rev. Letters* **102**, 1062804 (2009)

Figure Captions

Figure 1: The tunneling problem and its quantum computing gate equivalent. The scattering matrix associated to a device relates the incoming (a^+ , b^-) to the outgoing (a^- , b^+) wave amplitudes. It can be viewed as the matrix representing the rotation of a qubit from the initial state $|\psi(IN)\rangle$ to the final state $|\psi(OUT)\rangle$.

Figure 2: Bloch sphere representation of the effective spin (qubit) $|\psi(OUT)\rangle$. The radius of the sphere is equal to 1.

Figure 3: Transmission ($T = |t|^2$) and reflection ($R = |r|^2$) coefficients versus reduced wavevector \tilde{k} of electron incident on a single delta scatterer. The expressions for $|t|$ and $|r|$ are given by Equation (51) and (52), respectively.

Figure 4: Plot of the phase angles (φ, θ) associated to the spinor $|\psi(OUT)\rangle$ describing tunneling through a resonant tunneling structure as a function of the reduced wavevector $\tilde{k} = k/k_0$, where $k = \frac{1}{\hbar} \sqrt{2m^*E}$, E is the kinetic energy of the incident electron in the contact; $k_0 = m^*V_I/\hbar^2$, and V_I is the strength of the delta scatterer. The two delta scatterers are separated by 50\AA and have a strength $V_I = 0.3eV\text{\AA}$. $\Delta\tilde{k}$ is the minimum wavevector (in reduced units) needed to realize a spin flip from the south to north poles on the Bloch sphere. The zeroes in θ are the locations of the energy resonances.

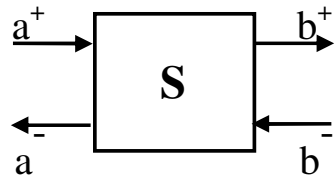
Figure 5: Transmission (T) and reflection (R) coefficients versus reduced wavevector \tilde{k} of the incident electron for a superlattice modeled as five delta scatterers of V_I separated by a distance a ($V_I = 0.3eV\text{\AA}$ and $a = 50\text{\AA}$). The curves labeled "1" and "2" are T versus \tilde{k} for two imperfect superlattices, i.e., for two arrays of 5 delta scatterers whose positions are selected uniformly over each interval of length 50\AA .

Figure 6: Reduced wavevector dependence of the phase angle (φ, θ) associated to the spinor $|\psi(OUT)\rangle$ describing tunneling across an array of five delta scatterers separated by 50\AA and with a scattering strength $V_I = 0.3eV\text{\AA}$. The zeroes in θ are where the transmission through the super-

lattice reaches unity. Also shown as dashed lines are the angles (φ, θ) through two random arrays of elastic scatterers.

Figure 7: Evolution of the angle θ for the spinor $|\psi(OUT)\rangle$ on the Bloch sphere as a function of sample length for two different arrays of elastic scatterers (two top curves). The smoother curve represents the average of θ calculated over an average of 10^5 arrays with the locations of each individual scatterer varied uniformly across each subsection of the array. The elastic mean free path Λ_{el} (in units of subsections crossed) is where $\bar{\theta} = \frac{\pi}{2}$.

Figure 8: Plot of the average over an ensemble of 10^5 impurity configurations of the conductance as a function of the number of impurities crossed in the sample. Also, shown is the value of the classical conductance calculated neglecting the effects of multiple reflections between scatterers. The elastic mean free path Λ_{el} (in units of subsections crossed) is where the Landauer conductance reaches a value of e^2/h .



	Tunneling Problem	Quantum Computing Analog
L → R		$ 0\rangle = \begin{bmatrix} 1 \\ 0 \end{bmatrix} \rightarrow \text{Q.C. Gate} \rightarrow \begin{bmatrix} t \\ r \end{bmatrix}$
R → L	<p>Figure 1: J. Wan et al</p>	

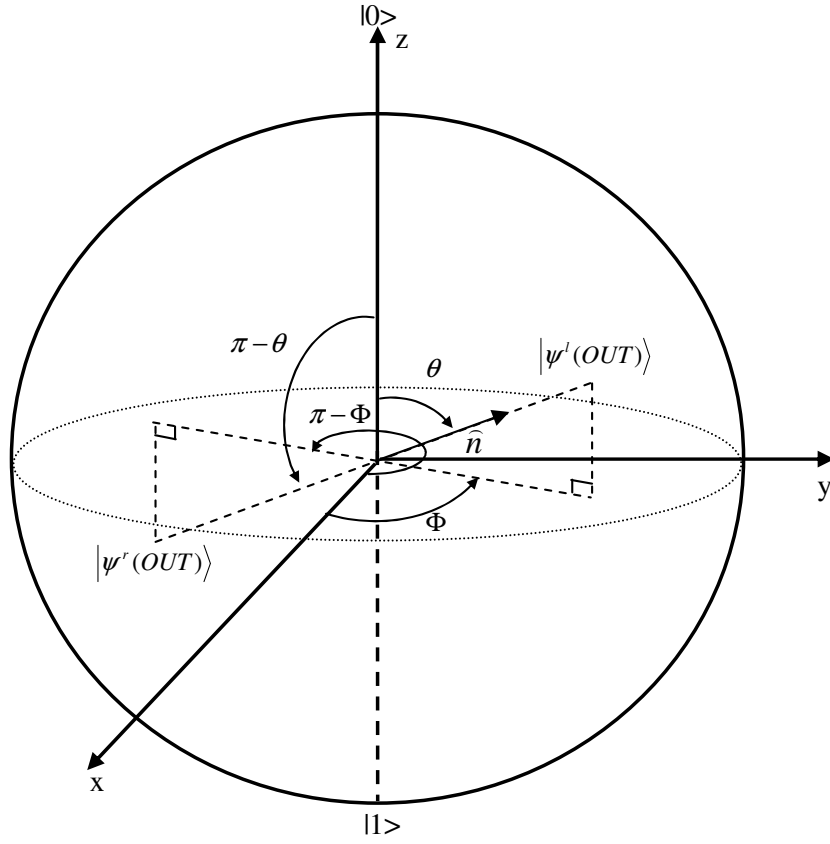


Figure 2: J. Wan et al

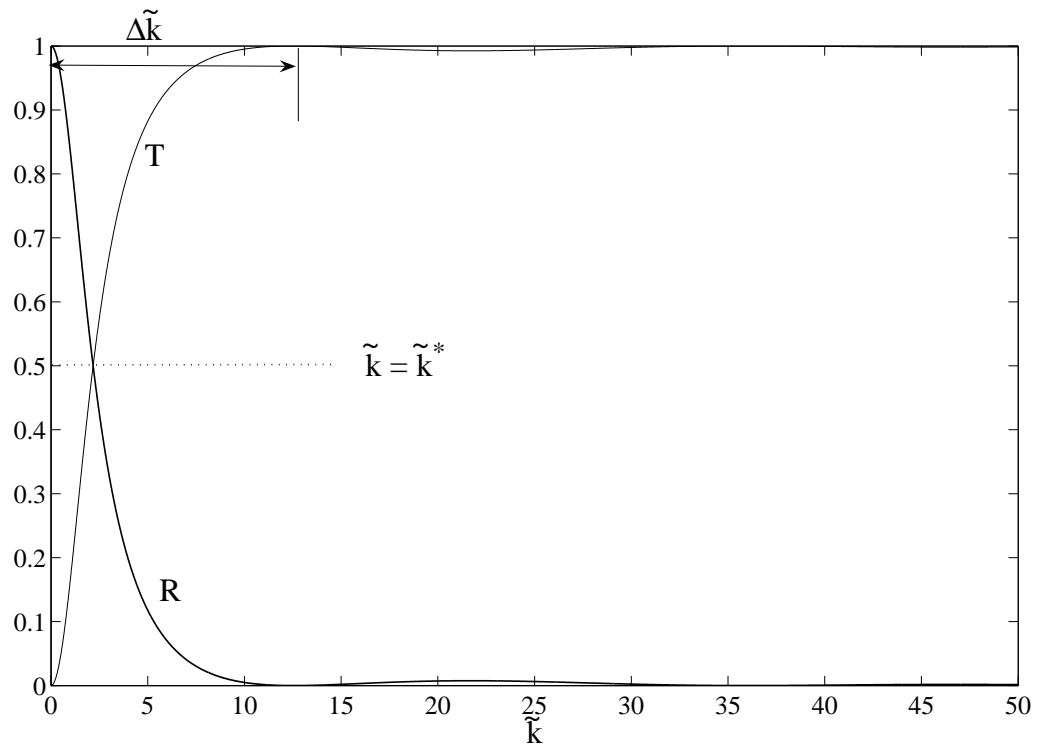


Figure 3: J. Wan et al

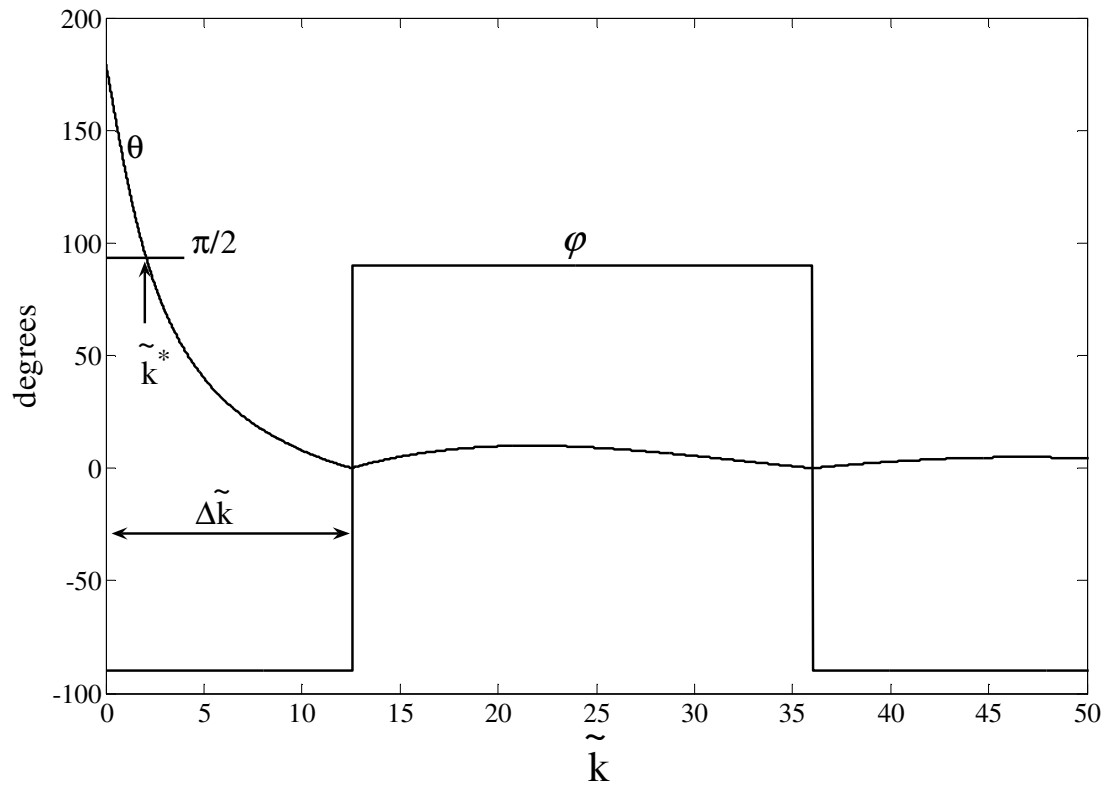


Figure 4: J. Wan et al

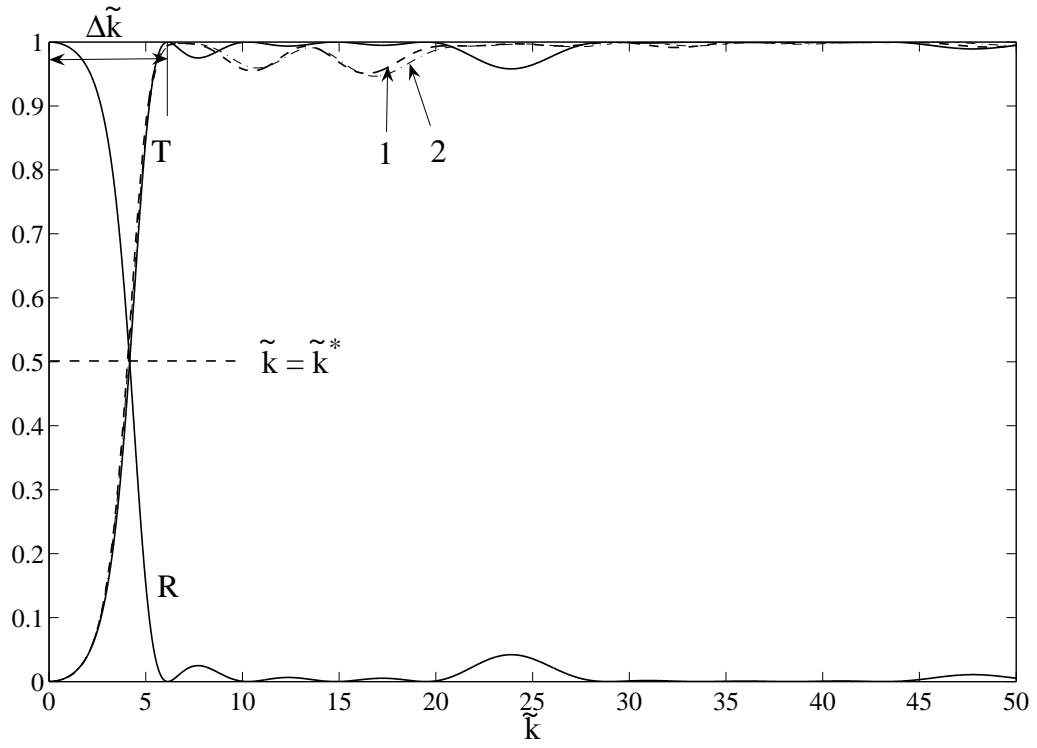


Figure 5: J. Wan et al

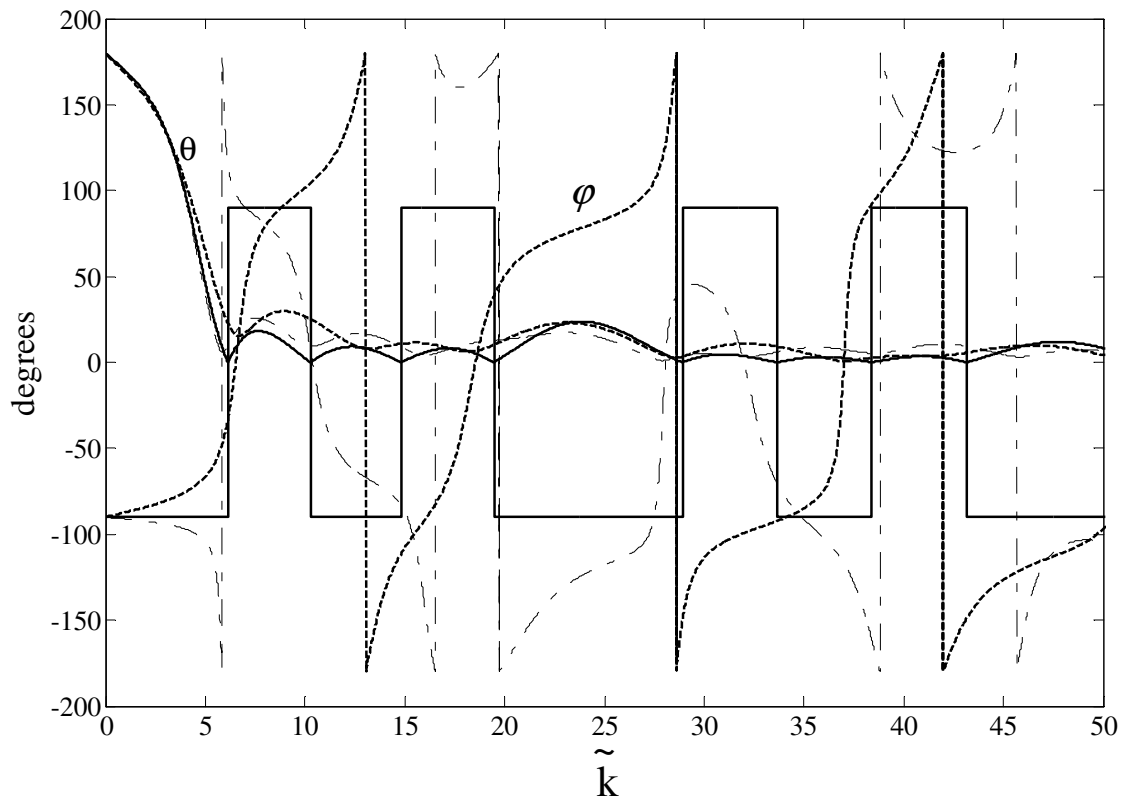


Figure 6: J. Wan et al

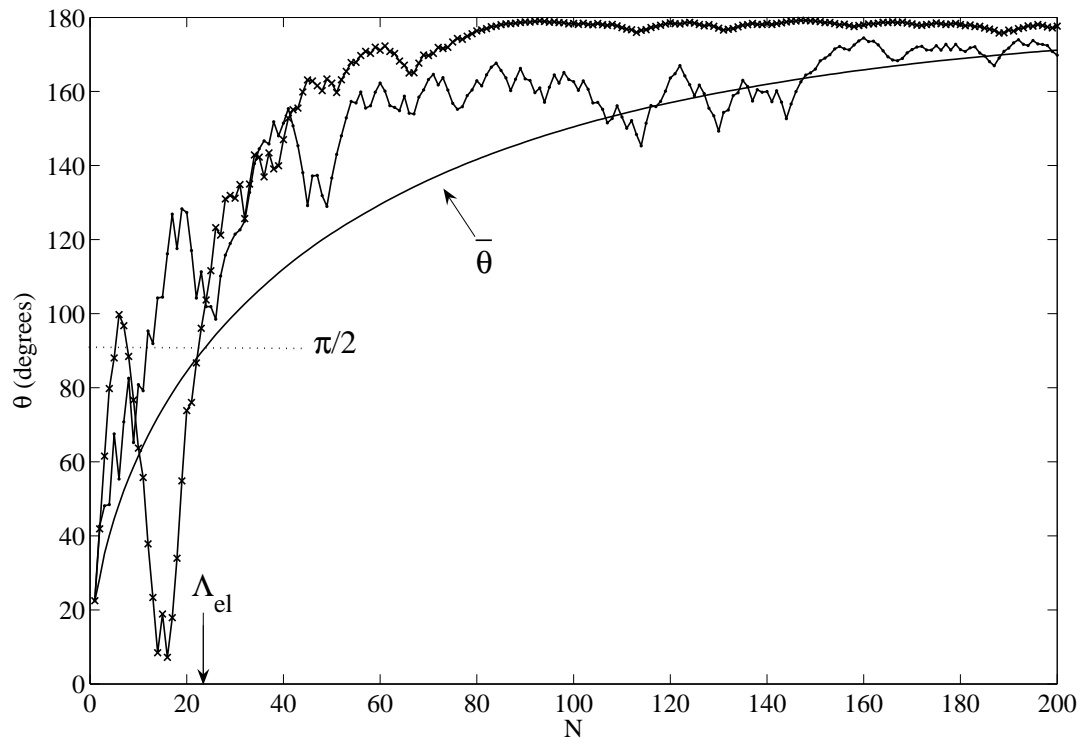


Figure 7: J. Wan et al

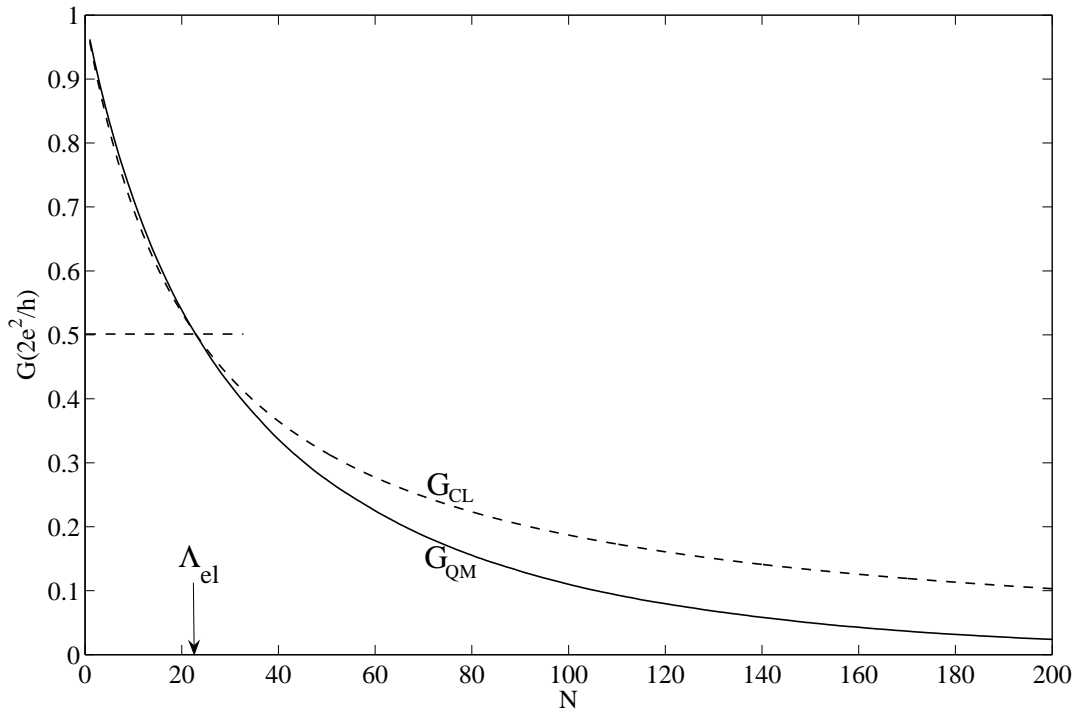


Figure 8: J. Wan et al